

CONTINUOUS REPOPULATION OF LYMPHOCYTE SUBSETS IN TRANSPLANTED MYCOBACTERIAL GRANULOMAS

H. A. Schreiber^{1,2,4}, J. S. Harding^{1,2,4}, C. J. Altamirano^{1,3}, O. Hunt¹,
P. D. Hulseberg^{1,2}, Zs. Fabry^{1,2} and M. Sandor^{1,2,3*}

¹Department of Pathology and Laboratory Medicine, University of Wisconsin,
School of Medicine and Public Health, Madison, WI 53706, USA

²Cellular and Molecular Pathology Training Program, University of Wisconsin

³Microbiology Doctoral Training Program, University of Wisconsin

⁴Co-First Authors

Granulomas are the interface between host and mycobacteria, and are crucial for the survival of both species. While macrophages are the main cellular component of these lesions, different lymphocyte subpopulations within the lesions also play important roles. Lymphocytes are continuously recruited into these inflammatory lesions via local vessels to replace cells that are either dying or leaving; however, their rate of replacement is not known. Using a model of granuloma transplantation and fluorescently labeled cellular compartments we report that, depending on the subpopulation, 10–80% of cells in the granuloma are replaced within one week after transplantation. CD4⁺ T cells specific for *Mycobacterium* antigen entered transplanted granulomas at a higher frequency than Foxp3⁺ CD4⁺ T cells by one week. Interestingly, a small number of T lymphocytes migrated out of the granuloma to secondary lymphoid organs. The mechanisms that define the differences in recruitment and efflux behind each subpopulation requires further studies. Ultimately, a better understanding of lymphoid traffic may provide new ways to modulate, regulate, and treat granulomatous diseases.

Keywords: *mycobacteria*, granuloma, cellular traffic, T cells, B cells, NK cells

Introduction

Properly formed *Mycobacterium*-induced granulomas protect an estimated two billion individuals from active disease by attenuating bacterial growth and dissemination [1]. These lesions are comprised of clustered, infected and noninfected macrophage and dendritic cells (DCs) surrounded by activated lymphocytes [2]. During acute mycobacterial infection, formation of the granuloma protects the host by containing the infection and localizing the dominant IFN γ -producing CD4⁺ T cell immune response [3]. As infection progresses into the chronic stage the granuloma protects the host by preventing bacterial dissemination, but also provide the mycobacteria with a long-term survival niche [4–6]. Recent studies have begun to demonstrate that granulomas are dynamic lesions that allow cells to migrate in and out. Cosma et al. have shown that super-infecting *Mycobacterium* species and infected macrophage preferentially home into pre-existing granulomas [7, 8]. On a cellular level, Egen and colleagues elegantly demonstrated the access of CD4⁺ T cells to pre-established granulomas and their incessant movement within the lesions [9]. We have previously shown that activated T cells traffic into preexisting mycobacterial granulomas during both influenza and LCMV co-infection, as well

as during autoimmune conditions [10–12]. Despite the understanding these insights have brought, many questions remain regarding cellular traffic in and out of granulomas [13].

Current methodology has not been sufficient to ask questions regarding the timing and proportion of traffic among different cellular subsets that both enter and exit granulomas, and so novel models have been needed. We have recently developed a model that involves grafting granuloma-containing liver from *Bacillus Calmette-guerin* (BCG)-infected mice under the kidney capsule of uninfected, syngeneic mice. Using this model, we reported that dendritic cells (DCs) traffic in and out of both acute and chronic granulomas (Schreiber et al. manuscript submitted). A continuously reforming granuloma structure is in agreement with recent studies demonstrating the continuous change and movement of granulomas using long-term CT/PET imaging. Proper granuloma formation relies on the recruitment and special organization of many lymphocyte populations. Although macrophage are the predominate cell in *Mycobacterium*-induced granulomas, lymphocytes, especially T cells, are crucial for the formation and maintenance of the lesions [14]. In the absence of CD4⁺ T cells, there is no proper granuloma formation [15–17]. Each lesion is comprised of a complex, heterogeneous T cell reper-

* Corresponding author: Matyas Sandor, 5468 MSC, 1300 University Ave, Madison, WI, USA 53705; Phone: 01-608-265-8715; E-mail: msandor@wisc.edu

toire [18] and while CD4⁺ T cells are crucial, CD8⁺ T cells also play an important role [19]. While the presence of regulatory T cells in the granuloma has been known, their role and effects are only beginning to be understood [20]. NK cells in the granuloma provide a critical secondary source of IFN γ [21] and B cells are thought to play a role in dampening inflammatory damage, as well as enhancing local immunity around the granuloma [22]. A question that remains unanswered about the complex coordination of these different cell types is the rate at which they are exchanged in the granulomatous lesions.

Here we demonstrate the feasibility of tracking a variety of cell populations into transplanted infected liver tissue including polyclonal CD4⁺, CD8⁺, B220⁺ and NK1.1⁺ cells, as well as *Mycobacterium*-specific CD4⁺ T cells. All of these cell types are important modulators in maintaining granuloma integrity, structure and function. Using this novel granuloma transplantation model, we have compared the exchange rate of different lymphocyte populations within lesions by measuring the ratio of donor and recipient cells at different time points. Data from this study shows that chronic granulomas are continuously restructured and the cellular subsets observed have access into chronic lesions during the one-week observational period. These findings demonstrate that not only does each of the investigated lymphocyte subsets have access to granulomas, but the rate of appearance among the different subpopulations in the transplanted lesions is different.

Results

Acute and chronic Mycobacterium-induced granulomas are comprised of many lymphocytic subsets

Our earlier work has demonstrated that dendritic cells have more access to chronic granulomas than to acute ones, an unanticipated finding (Schreiber et al. manuscript submitted). Here, we investigate the access of other cellular subsets into acute and chronic *Mycobacterium*-induced granulomas. In our BCG model these subsets are clearly distinguishable by flow cytometry at both 3 (acute) and 10-weeks (chronic) post infection (Fig. 1). CD4⁺ T cells comprise 5–10% of granuloma infiltrating cells and have proven to be indispensable for host protection and granuloma formation (Fig. 1 top row). CD8⁺ T cells are present at similar frequencies in the granuloma as CD4⁺ T cells and provide an additional source of IFN γ (Fig. 1 top row). When infected mice receive an adoptive transfer of 5×10^5 CFSE-labeled dsRED P25 CD4⁺ T cells, which have TCR specificity for *Mycobacterium* Ag85B of Mtb and BCG, those CD4⁺ cells have access to the granuloma (Fig. 1 middle row). Natural killer (NK) cells in BCG-induced granulomas are another source of protective IFN γ (Fig. 1 bottom row). The role of B cells, characterized here by B220⁺ expression, during mycobacterial infection remains largely unknown [23]. However, their high frequency and abun-

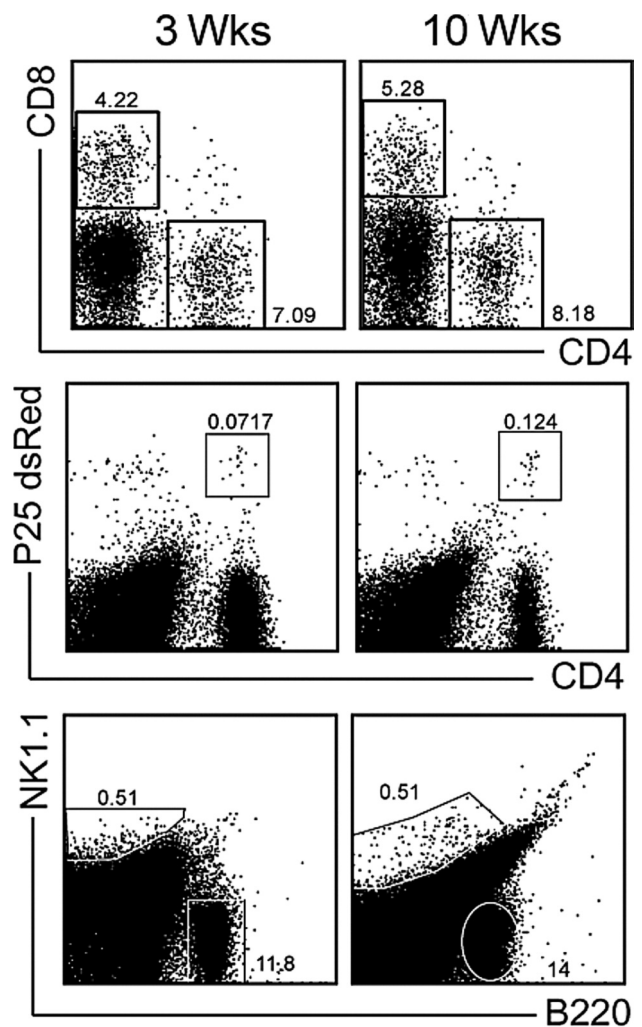


Fig. 1. Lymphocyte subsets in 3 and 10-week *Mycobacterium bovis* strain Calmette-Guerin-induced granulomas. C57BL/6 mice were systemically infected intraperitoneally with BCG. Three and ten weeks post-infection livers were harvested, and granuloma-infiltrating cells were isolated. For P25 experiments, 5×10^5 dsRed V β 11+CD4⁺ cells from the P25 Tg mouse were adoptively transferred into infected mice one week prior to harvest. FACS analysis of CD8⁺ and CD4⁺ (top row), P25 (middle row) and NK1.1⁺ and B220⁺ (bottom row) populations in liver granulomas. Subset gating scheme shown above is used throughout manuscript. Plots obtained from live cells gate of SSC versus FSC. Plots representative of at least 3–5 independent experiments

dance in acute, and even more so in chronic granulomas suggest they are an important subset to study (Fig. 1 lower plots). Flow cytometric plots presented here demonstrate the breadth of lymphocyte subsets in both acute and chronic *Mycobacterium*-induced granulomas. Though the role of these subtypes during infection is beginning to be understood, very little is known about the rate at which they enter lesions and are replenished by systemic sources. The gating scheme presented here will be used throughout to better understand their traffic.

Transplantation of granuloma-containing liver piece under the renal capsule of GFP recipients

To study cellular traffic, a small piece ($\sim 15 \pm 3$ mg) of liver from colorless uninfected, acutely (3 weeks) or chronically (10 weeks) infected mouse was transplanted underneath the kidney capsule of syngeneic GFP⁺ recipients (Fig. 2A). 1, 3 or 7 days post transplant the kidney was excised and visualized by fluorescent microscopy (Fig. 2B shows day 3). Cellular morphology and absence of many GFP⁺ cells easily identifies the colorless, transplanted liver specimen. GFP⁺ cells found in the transplanted graft are unequivocally of recipient origin. For the first time, this model allows the phenotyping and quantification of the migration of lymphocytic subsets into pre-existing acute and chronic mycobacterium-induced granulomas.

CD4⁺ T cells migrate into both acute and chronic granulomas with similar efficiency

Previous studies have demonstrated that non-*Mycobacterium* specific CD4⁺ T cells can enter pre-existing, acute

granulomas [9]. To retest their results using our transplantation model and test whether polyclonal CD4⁺ T cells also enter chronic lesions, we tracked the migration of this subset into transplanted granulomas using fluorescent microscopy and flow cytometry (Fig. 3). 1, 3 and 7 days post transplant the grafted kidney was excised. Frozen tissue sections were examined for CD4⁺ cellular migration into transplanted granulomas. Infiltrating, recipient CD4⁺ cells (R) were identified by GFP⁺ fluorescence, while transplanted donor CD4 (D) cells are GFP⁻ (Fig. 3A). A mean distribution was calculated after counting all CD4⁺ T cells in each lesion (Fig. 3B). By day 1 post transplant 2.5% ($\pm 2.5\%$) of total CD4⁺ T cells in a granuloma were of recipient origin. By days 3 and 7 post transplant the proportion of recipient CD4⁺ T cells of total CD4⁺ T cells in the granulomas increased to 13% ($\pm 3.5\%$) and then 35% ($\pm 4.7\%$), respectively, (Fig. 3B). Flow cytometry was used to investigate GFP⁺CD4⁺ cellular influx into the entire graft, which includes granuloma and non-granuloma tissue (Fig. 3C and D). The transplanted liver graft was excised from the kidney, homogenized and analyzed by flow cytometry (Fig. 3C upper panels). Flow cytometry analysis of the GFP fluorescence of the CD4⁺ population (Fig. 3C lower pan-

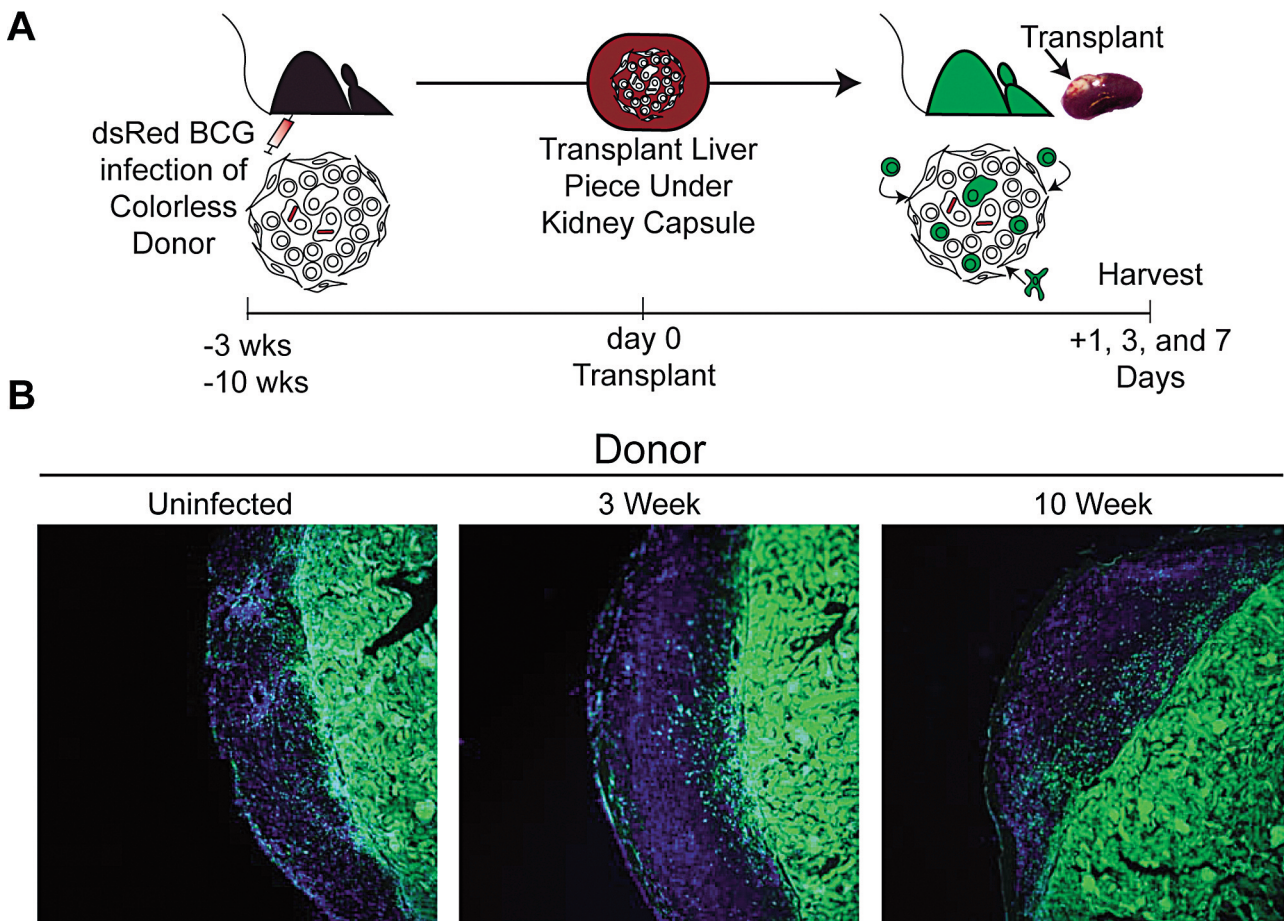


Fig. 2. Transplantation of uninfected, 3- and 10-week BCG infected colorless liver tissue under the kidney capsule of GFP recipient mice. **A**, Experimental Scheme. **B**, Fluorescent microscopy of kidney sections 3 days post transplant of uninfected, 3- and 10-week BCG infected colorless liver tissue. Images taken at $\times 10$ magnification. GFP (green) and DAPI nuclear stain (blue)

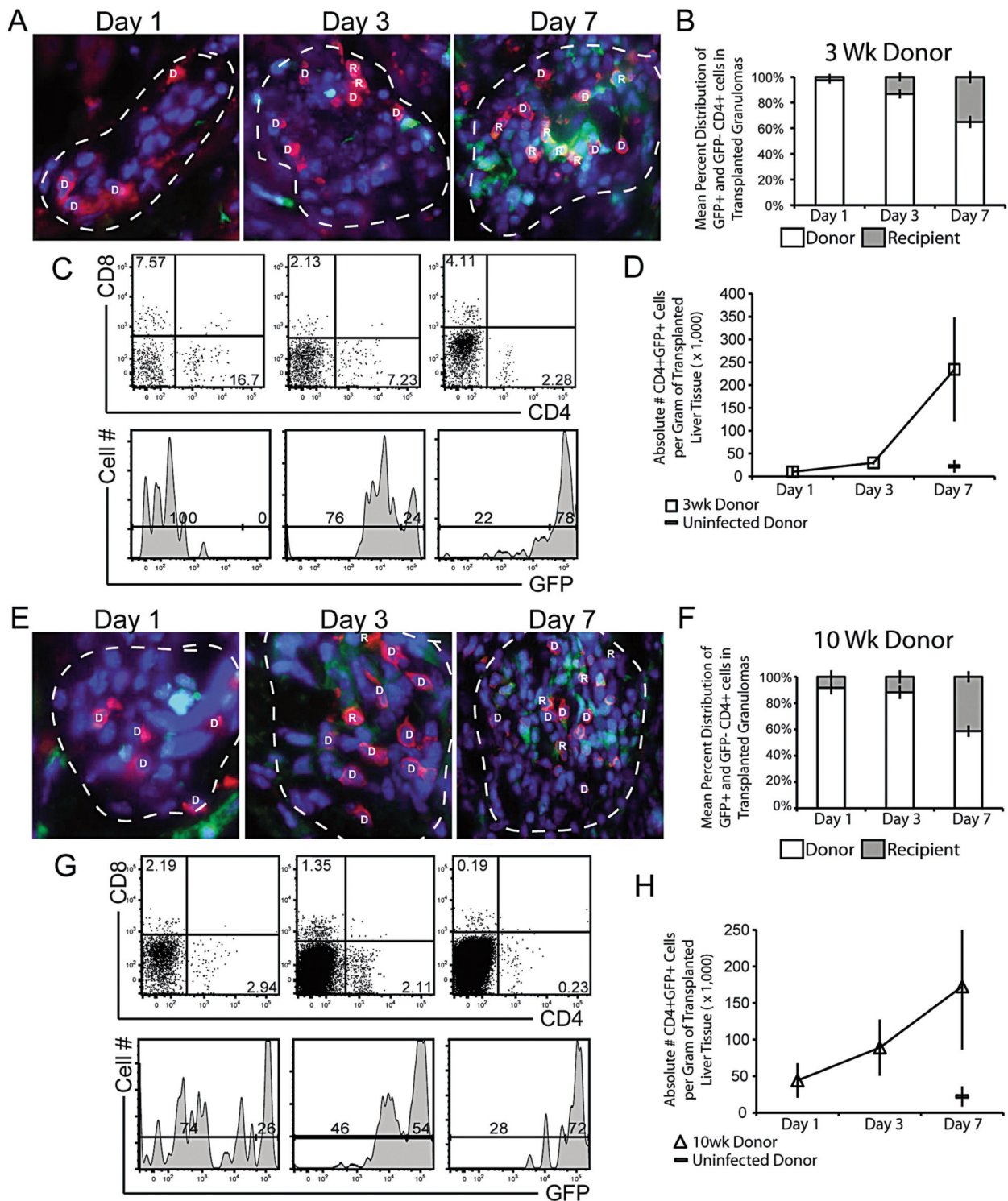


Fig. 3. Migration of recipient GFP+CD4+ T cells into transplanted granulomas in 3- and 10-week Mycobacterium-infected donor liver tissue. Liver tissue, containing granulomas from 3- (A–D) and 10-week (E–H) mycobacterial infection, was transplanted underneath the kidney capsule of uninfected GFP recipients. A & E, Digitally magnified $\times 1000$ fluorescent microscopy images taken of transplanted specimen 1, 3, and 7 days post transplant of 3- and 10-week BCG-infected donor liver. Granulomas outlined with white dashed lines, recipient cells (green), donor CD4 (red), recipient CD4 (orange/yellow) and DAPI nuclear stain (blue). Granuloma-associated CD4⁺ T cells were designated to be either donor (D) or recipient (R)-derived, based on CD4–GFP co staining. B & F, Mean distribution of all donor (white bars) and recipient (grey bars) CD4 T cells per granuloma 1, 3 and 7 days post transplant. CD4 distribution was determined from 10–15 granulomas per time point. C & G, 1, 3 and 7 days post transplant, transplanted donor liver tissue was excised and prepared for flow cytometry. Upper dot-plot panels, CD8 and CD4 surface staining. Lower histograms, GFP distribution of CD4⁺ gating shown in upper panels. Gating generated from GFP⁺ controls. D & H, Mean absolute number of infiltrating CD4⁺GFP⁺ T cells per gram of total transplanted tissue. Data generated from 2–3 independent experiments; error bars represent SEM

els) reveals a faster, more pronounced infiltration and replacement of recipient CD4⁺ T cells into the transplanted granulomas than microscopy. 3 and 7 post transplant 24% and 78% of total CD4⁺ T cells in the entire transplanted piece are of recipient origin, respectively (Fig. 3C lower panel). The difference in CD4⁺ T cell migration previously observed (Fig. 3A and B) may be due to antigenic specificity. While many non-specific CD4⁺ T cells may be recruited to the transplant, only a portion of them likely enter granulomas. The measured difference may also result from the fact that most donor CD4⁺ T cells are localized in granulomas. When extra-granulomatous tissue is included in the measurement, recipient CD4⁺ cells make up a larger majority. Compared to infected donor tissue, fewer CD4⁺ T cells are recruited into uninfected donor tissue 7 days after transplant (Fig. 3D) suggesting that recruitment and migration of CD4⁺ T cells into the transplanted tissue and granulomas is not an artifact of the transplantation procedures.

Our previous studies demonstrated that chronic granulomas are quickly and intensely surveyed by dendritic cells following transplantation (Schreiber et al. manuscript submitted). Based on this observation, we then tested if CD4⁺ T cells had similar access to chronic granulomas (Fig. 3E–H). Fluorescent microscopy analysis of all CD4⁺ T cells in transplanted granulomas 1, 3 and 7 days post transplanted showed that 8% ($\pm 4.9\%$), 12% ($\pm 5\%$) and 41% ($\pm 4.3\%$) were of donor origin, respectively (Fig. 3E and F). These data demonstrate that, like dendritic cells, CD4⁺ T cells also have access to chronic lesions. As with CD4⁺ migration into acutely infected tissue, analysis by flow cytometry showed more total CD4⁺ T cell migration into chronically infected transplanted tissue than migration into transplanted granulomas alone (Fig. 3G). Since CD4 T-cells migrated into transplanted tissue from chronically infected mice, but not uninfected tissue, migration is not a procedural artifact (Fig. 3H). These data demonstrate that CD4⁺ T cells migrate into acute and chronic *Mycobacterium*-infected donor tissue, and into pre-established granulomas, although at a lower frequency.

Mycobacterium Ag85B-specific CD4⁺ T cells readily migrate into both acute and chronic granulomas

We next investigated if antigen specificity was involved in migration of CD4⁺ T cells into granulomas, which could compensate for differences observed between local granuloma influx and increased global tissue transplant influx. We transplanted donor tissue into Thy1.1 P25 CD4⁺ T cell transgenic mice. Staining with anti-CD4 and anti-Thy1.1 identifies both donor (D) and recipient P25 (R) CD4⁺ T cells 7 days post transplant (Fig. 4A). When quantified, 49% ($\pm 7.8\%$) and 54% ($\pm 6.8\%$) of total CD4⁺ T cells in 3- and 10-week granulomas, respectively, were Thy1.1⁺ of recipient origin (Fig. 4B). These data suggest that P25 CD4⁺ T cells enter 3 and 10-week lesions more quickly and at slightly higher frequencies than a polyclonal population. Flow cytometry of whole transplant pieces revealed similar

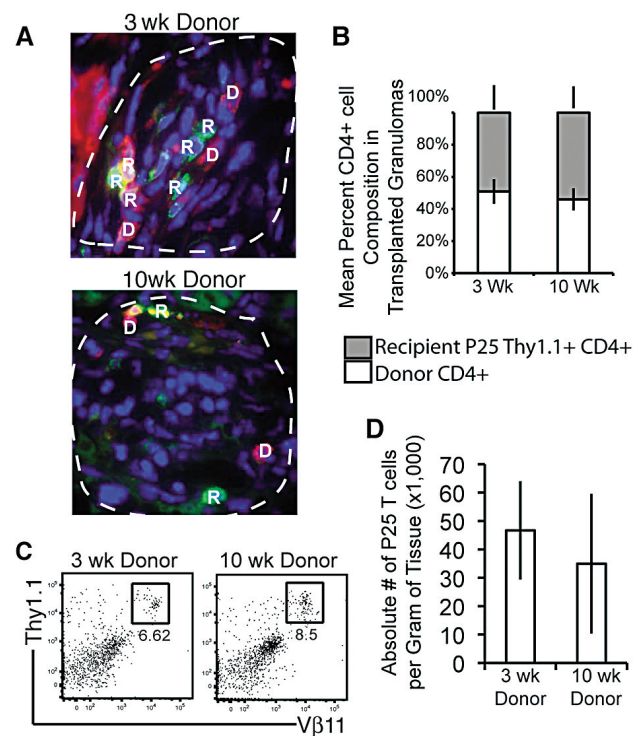


Fig. 4. Migration of Thy1.1 P25 CD4⁺ T cells into 3- and 10-week infected donor tissue.

Briefly, Thy1.2 C57Bl/6 liver tissue

from 3- and 10-week infected mice was transplanted under the kidney capsule of P25 Thy1.1 Tg recipients.

A, Fluorescent microscopy images of transplanted kidney

7 days post transplant. Images digitally magnified from images taken at $\times 1000$ magnification white-dashed line indicates border of granuloma. Red indicates donor anti-CD4

surface stain (D), and green or yellow/orange indicate recipient Thy1.1⁺ cells (R). **B**, Mean percent composition

of donor CD4⁺Thy1.1⁻ cells (white bars) and recipient CD4⁺Thy1.1⁺ cells (grey bars) in transplant granuloma.

C, 7 days later donor tissue was removed and stained with anti-Thy1.1 and V β 11 to locate Tg T cells.

D, Absolute number of infiltrating P25+ cells

per gram of transplanted tissue. Error bars indicate \pm SEM

rates of P25 Tg T cell migration into both 3- and 10-week infected donor grafts (Fig. 4C), nor were there differences in the absolute number of P25 T cells per gram donor tissue between 3 and 10-week infected transplants

Foxp3⁺ regulatory T cells traffic into acute and chronic granulomas at a similar rate and frequency, but to a lesser extent than conventional CD4⁺ T cells

Infection of Foxp3-GFP reporter mice with BCG shows that Foxp3⁺ regulatory T cells are present in acute and chronic granulomas, though in smaller numbers than CD4 or CD8 (Fig. 5A). To track regulatory T cell migration into granulomas, liver tissue from 3- and 10-week infected colorless mice was transplanted under the kidney capsule of Foxp3-GFP reporter recipients (Fig. 5B). Within one week, Foxp3⁺ regulatory T cells entered acute and chronic gran-

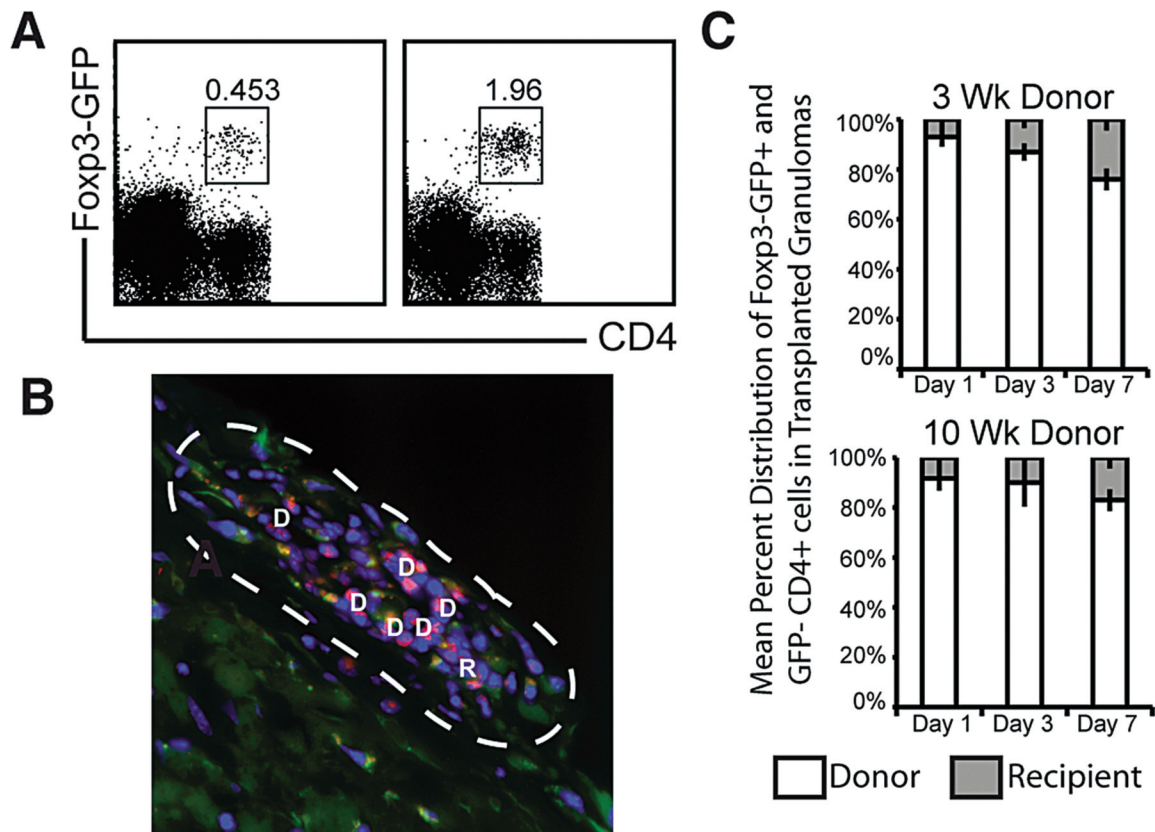


Fig. 5. Migration of regulatory T cells into 3- and 10-week infected donor tissue. **A**, FACs plot of three (left plot) and ten (right plot) week infected Foxp3-GFP reporter mice. **B**, Liver tissue from 3-week infected colorless mice was transplanted under the kidney capsule of Foxp3-GFP reporter recipients. Fluorescent microscopy image of transplanted kidney 7 days post transplant. Image digitally magnified from images taken at $\times 1000$ magnification white-dashed line indicates border of granuloma. Red indicates donor anti-CD4 surface stain (D), and green or yellow/orange indicate recipient Foxp3⁺ cells (R). **C**, Mean percent composition of donor CD4⁺GFP⁻ cells (white bars) and recipient CD4⁺Foxp3-GFP⁺ cells (grey bars) in transplant granuloma

ulomas at a similar rate and frequency (Fig. 5C). However, compared to conventional CD4⁺ T cells, recruitment of regulatory Foxp3⁺ T cells was much lower.

Other lymphocytes, including CD8⁺, B220⁺ and NK1.1⁺ subsets, also demonstrate high cellular turnover within both acute and chronic granulomas by one week

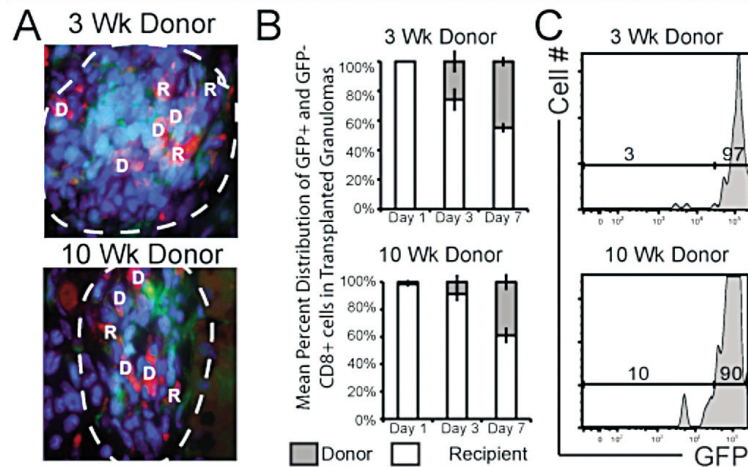
Thus far, our data demonstrates an active recruitment of CD4⁺ T cells (polyclonal and *Mycobacterium*-specific) into both acute and chronic granulomas (Figs 3 and 4). To test if other lymphocytic compartments also migrate into transplants, we used the same methodology to analyze CD8⁺, B220⁺ and NK1.1⁺ populations (Fig. 6). Cell specific influx into individual granulomas was measured by fluorescent microscopy of donor GFP⁻ (D) and recipient GFP⁺ (R) cells (Fig. 6A's). Like CD4⁺ T cells, CD8⁺ T cells exhibited a gradual turnover within 3- and 10-week granulomas, reaching levels of 45% ($\pm 3.1\%$) and 39% ($\pm 5.7\%$), respectively, by one week after transplant (Fig. 6B CD8⁺). As with the CD4⁺ population, recipient CD8⁺ cells made up a higher proportion of total CD8 cells in the entire graft when compared to the distribution in the granuloma (Fig. 6C CD8⁺).

B220 migration into acute granulomas was much lower than migration into chronic granulomas: 30% ($\pm 4.4\%$) compared to 67% ($\pm 3.7\%$), respectively ($p < 0.0001$) (Fig. 6, B220⁺ A and B). Previous data (Fig. 1) demonstrates the progressive accumulation of B220⁺ cells, which supports the distribution measured here. The increase in the B220⁺ population as infection proceeds into the chronic stage may have significance and warrants future investigation. The NK1.1⁺ population showed the smallest turnover of any subset, with recipient NK1.1⁺ cells comprising 20% ($\pm 5.9\%$) and 32% ($\pm 5.1\%$) of 3 and 10-week granulomas, respectively (Fig. 6, NK1.1⁺ A and B). Unlike CD4⁺ and CD8⁺ populations, the proportion of infiltrating B220 and NK1.1 to total B220 and NK1.1 cells is similar in both the graft and granulomas alone (Fig. 6, B220⁺ and NK1.1⁺ C's) suggesting that their migration into the transplant is directed more specifically to granulomatous lesions.

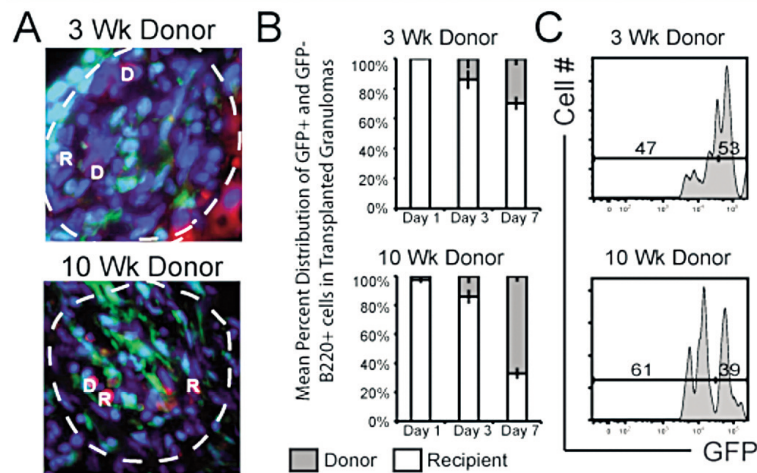
Few CD4⁺ and CD8⁺ T cells migrate out of acute and chronic granulomas

While the traditional paradigm is that most lymphocytes are retained and eventually die in the granuloma, we used our model to show and measure T lymphocytes efflux out

CD8+



B220+



NK1.1+

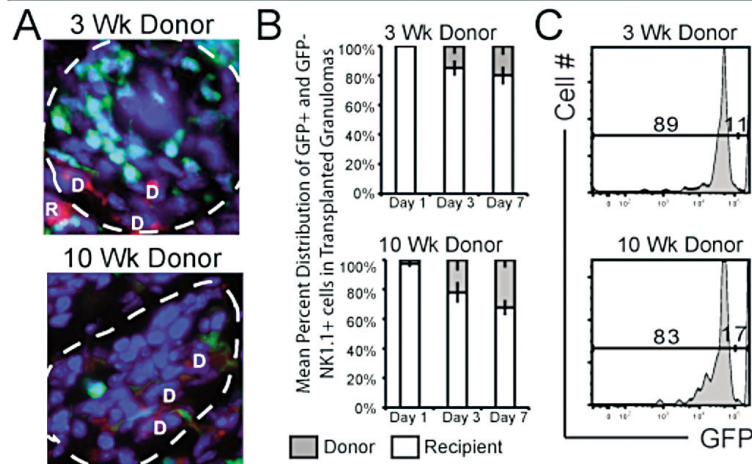


Fig. 6. Migration of recipient GFP+ CD8+ T cells, NK1.1+ and B220+ cells into transplanted granulomas within 3- and 10-week Mycobacterium-infected donor liver tissue. Analysis of GFP+ cellular migration into transplanted 3- and 10-week granuloma-containing infected donor liver tissue was performed in the same way as CD4+ analysis in Fig 3.

A, Digitally magnified $\times 1000$ fluorescent microscopy images taken of transplanted specimen 7 days post transplant of 3- and 10-week BCG-infected donor liver. **B,** Mean percent distribution of GFP+ (R) and GFP- (D) CD8+ T cells, NK1.1+ and B220+ in transplanted granulomas. **C,** GFP distribution of CD8+ T cells, NK1.1+ and B220+ gated population shown in Fig. 1 at day 7 post transplant. Data generated from 2–3 independent experiments; error bars represent SEM

of acute and chronic transplanted granulomas (Fig. 7A). For these studies, liver from 3-, 6- and 10-week infected GFP⁺ mice were transplanted into syngeneic, colorless recipients, allowing us to track GFP⁺ cellular migration out of the transplanted granulomas. Tissue sections from the recipients' cervical lymph node (cLN), draining renal lymph node (rLN) and spleen were stained for CD4 (Fig. 7B). While some GFP⁺ cells found in recipient organs were CD4⁺ (Fig. 7B right images), the majority of GFP⁺ cells did not co-stain, but were instead found in close proximity to CD4⁺ cells (Fig. 7B left and middle images). In addition to CD4⁺ T cells, CD8 staining of the rLN also revealed GFP⁺CD8⁺ cells (Fig. 7C left image, dashed arrow), as well

as GFP⁺CD8⁻ cells in close proximity to CD8⁺ cells (Fig. 7C middle and right images). The presence of fluorescent overlay at the point of contact between GFP⁺CD8⁻ cells and GFP⁺CD8⁺ resembles an immunological synapse (Fig. 7C yellow arrow), suggesting that GFP cells from the transplanted granulomas are a migratory antigen presenting cells (APC) like DCs (though unlikely to be macrophages since they are not very motile by nature). Using flow cytometry to track GFP⁺ cellular egression confirmed that very few cells leave the granuloma (data not shown). Based on the absolute number of T lymphocytes present in the grafted infected tissue and the number of GFP⁺ cells detected in secondary lymphoid organs by flow cytometry, approxi-

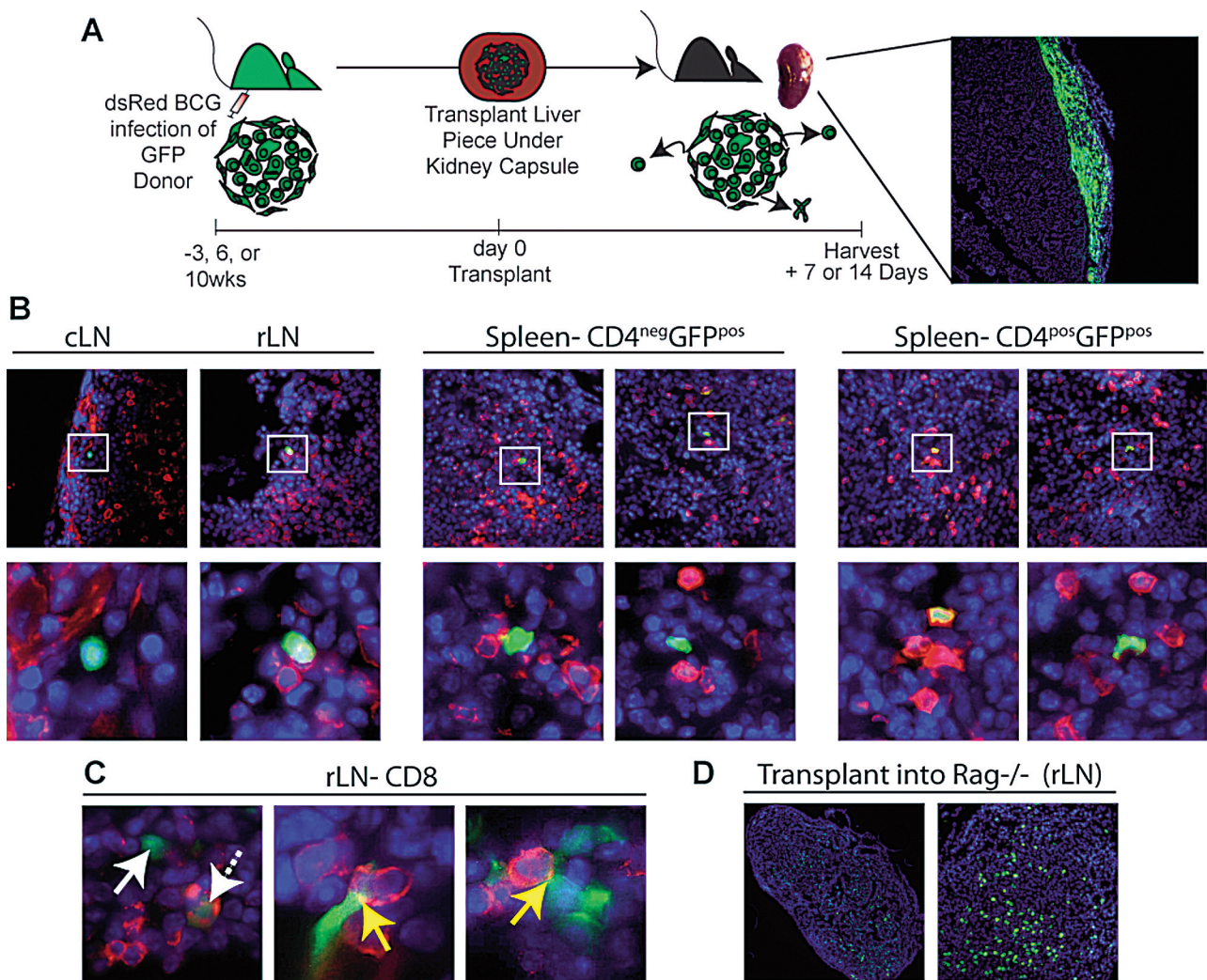


Fig. 7. Transplantation of 3- and 10-week BCG infected GFP liver tissue under the kidney capsule of colorless recipient mice.

A, Experimental Scheme. Briefly, Liver specimen (~0.15±3 mg) containing granulomas from a 3-, 6- or 10-week dsRED BCG infected GFP donor mouse is transplanted underneath the kidney capsule of colorless wildtype or Rag^{-/-} recipients. **B**, To track cellular migration out of transplanted granulomas, frozen sections from cLN, rLN and spleen 7 days post transplant were analyzed by fluorescent microscopy images.

C, Sections after transplant of a 6-week infected donor were stained for CD4 cells (red). Upper images taken at ×1000, lower images digitally zoomed in of region indicated by white box. Far right images of spleen demonstrate CD4+GFP+ co-staining, while middle and far left images do not. rLN sections from 3-week infected donor were stained with CD8 (red). Images taken at ×1000 and digitally magnified. Far right image, solid white arrow points to GFP+CD8- and dashed arrow points to GFP+CD8+ cell. Middle and right images, yellow arrows point to synapse-like co-staining of GFP+CD8- and CD8+ cell.

D, draining rLN 2 weeks after 3-week infected GFP donor liver piece was transplanted into Rag^{-/-} recipient. Images taken at ×10 and ×40, respectively

mately 1% and 5% of T cells leave the acute and chronic granulomatous tissue, respectively, by one week after transplant. To demonstrate that transplanted granulomas maintain their integrity and release few cells, we created a scenario that resulted in granuloma disruption. Here, infected liver from a GFP infected donor is transplanted under the kidney capsule of a colorless, Rag^{-/-} recipient. The recipient's inability to replenish the granuloma with new lymphocytes causes the granuloma to disintegrate, thereby releasing many GFP⁺ cells (Fig. 7D draining rLN). These data demonstrate that lymphocyte recruitment is crucial for retention of granuloma cells in the transplant and maintaining long-term granulomatous lesions.

Discussion

Granuloma formation is required by the host to control infection and by the pathogen to ensure its long-term survival and ability to transmit disease. Their dynamic structure is maintained by the recruitment of lymphocytes via nearby vessels through a chemokine gradient. Repopulating the granuloma with newly-recruited inflammatory cells is necessary to maintain granuloma integrity since most of the effector lymphocytes are not long-lived. The importance of this continuous repopulation is demonstrated in cases where the systemic lymphocyte pool is depleted, resulting in the disintegration of granulomas and reactivation of mycobacteria (i.e. HIV, SIV) [24, 25]. However, the rate and frequency at which this repopulation takes place is not known.

The granuloma transplantation model presented here is a new method to study the repopulation and egression of lymphocytes in the granuloma. Using GFP-expressing mouse strains, we are able to measure and track these exchanges. Collectively, the data presented here demonstrates that all observed lymphocyte populations are exchanged in both acute and chronic granulomas, but the rate and extent of their exchange differs between subpopulations. The recruitment of *Mycobacterium*-specific and non-specific CD4⁺ T cells into established granulomas has been demonstrated [11, 18]. However, this is the first report to show that within one week, approximately 30% of CD4⁺ T cells are coming from systemic sources. While flow cytometry analysis demonstrates the infiltration of GFP⁺ cells into the transplant, fluorescent microscopy analysis shows the ratio of systemic and transplanted cells on a granuloma-specific level. The data clearly demonstrates that both acute and chronic lesions are permissible to incoming cells. There is a higher frequency of infiltrating NK and B cells in chronic lesions compared to acute lesions, while a similar frequency of infiltrating T lymphocytes in both acute and chronic lesions. CD4⁺ T cells specific for mycobacterial antigen 85B (P25) are recruited at a higher frequency than polyclonal CD4⁺ T cells, which may be due to their antigen specificity or potentially a shorter lifespan. Conversely, regulatory Foxp3⁺ CD4⁺ T cells, which are also present in the granuloma, repopulate from systemic sources at a much lower frequency compared to conventional CD4⁺ T cells. These

data collectively demonstrate that the extent of exchange between the different CD4⁺ T cell populations with recipient's cells in the transplanted granuloma differs. Interestingly, the highest level of exchange was observed in the B cell population during chronic infection, with 80% of B cells being of recipient-origin by 7 days post transplant. The significance and mechanisms behind the different extents of repopulation of the different lymphocyte subpopulations will require future studies.

Our data also demonstrates that with the exception of a very small population, most lymphocytes do not leave the granuloma. This raises the question as to whether those cells that do leave the granuloma have an effect on the course of infection. The continuous rebuilding of the granuloma may provide an opportunity to modulate these sites. Therefore, a better understanding of granuloma maintenance, particularly in regards to repopulation, will be an important future direction of study.

Materials and Methods

Mice

GFP C57BL/6 (H2^b), Foxp3-GFP and C57BL/6 Rag^{-/-} mice were purchased from Jackson Laboratory (Bar Harbor, ME). P25 transgenic mice were a generous gift from Drs. Rothfuchs and Sher (NIH, Bethesda, MD). Mice were housed and bred in a pathogen-free facility at the University of Wisconsin Animal Care Unit (Madison, WI), according to the guidelines of the Institutional Animal Care and Use Committee.

Infection

Kanamycin-resistant dsRED-expressing BCG, a generous gift from Dr. Lalita Ramakrishnan (University of Washington, WA), was grown in Middlebrook 7H9 supplemented with 0.05% Tween 80 and 10% oleic acid-dextrose-catalase supplement (Difco, Detroit, MI) in the presence of kanamycin (50 µg/mL) and stored at -80°C. For infections, ampoules were thawed, diluted in PBS, and briefly sonicated to obtain single-cell suspensions. For systemic infection, a non-lethal dose of 1×10⁷ CFU in 100 µL is injected i.p.

Transplant

Mice were anesthetized by i.p. injection of a ketamine (90 mg/kg)/xylazine (10 mg/kg) mixture and s.c. injected with meloxicam for pain management. An area on the dorsal side of the mouse towards the posterior end was shaved and swabbed with iodine. A 1 cm longitudinal incision through the skin and peritoneum was made above last rib and hip joint, and the kidney then withdrawn. A 1 mm incision along the kidney capsule was made and the capsule then drawn away from the kidney creating an open pocket be-

tween the organ and the capsule. Two pieces of donor liver approximately 15 ± 3 mg in mass were inserted under the capsule. The peritoneum was then sutured and skin incision closed with surgical staples. Mice received kanamycin (5 mg/kg) in their water 1 day prior to surgery and for the duration of their recovery.

Mononuclear cell isolation and flow cytometry

Transplanted liver tissue was processed between two glass slides and treated with 5 mg/ml type I collagenase (Sigma-Aldrich, St. Louis, MO) at 37°C for 40 min with shaking. The softened granulomas were disrupted by repeated expulsion through a syringe for 1 minute and washed. Isolated cells were processed for flow cytometry. A total of 10^6 cells were incubated for 30 min on ice with saturating concentrations of labeled Abs with 40 µg/mL unlabeled 2.4G2 mAb to block binding to Fc receptors and washed 3 times with staining buffer (PBS plus 1% BSA). Fluorochrome-labeled Abs against NK1.1 (PK136), Vβ11 (RR3-15), Thy1.1 (OX-7), CD4 (RM4.5) and CD8 (53-6.7) were purchased from BD Biosciences (San Jose, CA). B220 (RA3-6B2) PE labeled was purchased from eBioscience (San Diego, CA). Anti-CD16/CD32 (2.4G2) was produced from a hybridoma. Cell surface staining was acquired on a FACSCalibur or LSRII (BD Biosciences, San Jose, CA) and analyzed with FlowJo (Tree Star) software version 5.4.5.

Fluorescent microscopy

Organs fixed over night in 3% formalin/25% sucrose in PBS were frozen down in O.C.T Compound (Tissue-Tek Sakura, Torrance, CA). 5–10 µm thick cryosections were cut from O.C.T-embedded tissue samples and fixed for 10 min in ice-cold acetone, then washed three times with PBS and outlined with a Pap pen. Sections were then surface stained, which included 40 µg/mL of 2.4G2 blocking Ab, for two hours at room temperature in PBS and washed with PBS for 30 minutes. Sections were mounted using ProLong Gold antifade reagent with DAPI (Invitrogen, Carlsbad, CA). All images were acquired with a camera (Optronics Inc., Goleta, CA) mounted on a fluorescence microscope (Olympus BX41, Leeds Precision Instruments). Picture-Frame software (Optronics Inc.) was used to obtain JPEG images.

Adoptive transfer

Pooled splenocytes and lymphocytes from dsRed P25 transgenic mice were CFSE labeled (Molecular Probes). 5×10^5 dsRed+CD4+ transgenic cells were adoptively transferred i.v. via retro-orbital injection into recipient mice 7 days prior to harvest.

Acknowledgements

We would like to thank Toshi Kinoshita for expert histopathology services, and members of our laboratory for helpful discussions and constructive criticisms of this work. Special thanks to Dr. Lalita Ramakrishnan (University of Washington) for her generous gift of the dsRED BCG plasmid and Drs. Rothfuchs and Sher (NIH, Bethesda, MD) for their generous gift of the P25 mice. Work supported by the Bill and Melinda Gates Foundation, and National Institutes of Health funding R01-A1048087 and R21-A1072638 (M. Sandor).

References

- Ulrichs T, Kaufmann SH: New insights into the function of granulomas in human tuberculosis. *J Pathol* 208, 261–269 (2006)
- Co DO et al.: Mycobacterial granulomas: keys to a long-lasting host-pathogen relationship. *Clin Immunol* 113, 130–136 (2004)
- Flynn JL et al.: An essential role for interferon gamma in resistance to Mycobacterium tuberculosis infection. *J Exp Med* 178, 2249–2254 (1993)
- Volkman HE et al.: Tuberculous granuloma formation is enhanced by a mycobacterium virulence determinant. *PLoS Biol* 2, e367 (2004)
- Schreiber HA et al.: Dendritic cells in chronic mycobacterial granulomas restrict local anti-bacterial T cell response in a murine model. *PLoS One* 5, e11453 (2010)
- Russell DG: Who puts the tubercle in tuberculosis? *Nat Rev Microbiol* 5, 39–47 (2007)
- Cosma CL, Humbert O, Ramakrishnan L: Superinfecting mycobacteria home to established tuberculous granulomas. *Nat Immunol* 5, 828–835 (2004)
- Cosma CL et al.: Trafficking of superinfecting Mycobacterium organisms into established granulomas occurs in mammals and is independent of the Erp and ESX-1 mycobacterial virulence loci. *J Infect Dis* 198, 1851–1855 (2008)
- Egen JG et al.: Macrophage and T cell dynamics during the development and disintegration of mycobacterial granulomas. *Immunity* 28, 271–284 (2008)
- Co DO et al.: Interactions between T cells responding to concurrent mycobacterial and influenza infections. *J Immunol* 177, 8456–8465 (2006)
- Hogan LH et al.: Virally activated CD8 T cells home to Mycobacterium bovis BCG-induced granulomas but enhance antimycobacterial protection only in immunodeficient mice. *Infect Immun* 75, 1154–1166 (2007)
- Sewell DL et al.: Infection with Mycobacterium bovis BCG diverts traffic of myelin oligodendroglial glycoprotein autoantigen-specific T cells away from the central nervous system and ameliorates experimental autoimmune encephalomyelitis. *Clin Diagn Lab Immunol* 10, 564–572 (2003)
- Davis JM, Ramakrishnan L: “The very pulse of the machine”: the tuberculous granuloma in motion. *Immunity* 28, 146–148 (2008)
- Co DO et al.: T cell contributions to the different phases of granuloma formation. *Immunol Lett* 92, 135–142 (2004)

15. Kaufmann SH, Ladel CH: Role of T cell subsets in immunity against intracellular bacteria: experimental infections of knock-out mice with *Listeria monocytogenes* and *Mycobacterium bovis* BCG. *Immunobiology* 191, 509–519 (1994)
16. Ladel CH et al.: Protective role of gamma/delta T cells and alpha/beta T cells in tuberculosis. *Eur J Immunol* 25, 2877–2881 (1995)
17. Mogues T et al.: The relative importance of T cell subsets in immunity and immunopathology of airborne *Mycobacterium tuberculosis* infection in mice. *J Exp Med* 193, 271–280 (2001)
18. Hogan LH et al.: *Mycobacterium bovis* strain bacillus Calmette-Guerin-induced liver granulomas contain a diverse TCR repertoire, but a monoclonal T cell population is sufficient for protective granuloma formation. *J Immunol* 166, 6367–6375 (2001)
19. Flynn JL et al.: Major histocompatibility complex class I-restricted T cells are required for resistance to *Mycobacterium tuberculosis* infection. *Proc Natl Acad Sci USA* 89, 12013–12017 (1992)
20. Ozeki Y et al.: Transient role of CD4+CD25+ regulatory T cells in mycobacterial infection in mice. *Int Immunol* 22, 179–189 (2010)
21. Smith D et al.: T-cell-independent granuloma formation in response to *Mycobacterium avium*: role of tumour necrosis factor-alpha and interferon-gamma. *Immunology* 92, 413–421 (1997)
22. Maglione PJ, Xu J, Chan J: B cells moderate inflammatory progression and enhance bacterial containment upon pulmonary challenge with *Mycobacterium tuberculosis*. *J Immunol* 178, 7222–7234 (2007)
23. Cooper AM: Cell-mediated immune responses in tuberculosis. *Annu Rev Immunol* 27, 393–422 (2009)
24. Scanga CA et al.: Depletion of CD4(+) T cells causes reactivation of murine persistent tuberculosis despite continued expression of interferon gamma and nitric oxide synthase 2. *J Exp Med* 192, 347–358 (2000)
25. Aagaard C et al.: Protection and polyfunctional T cells induced by Ag85B-TB10.4/IC31 against *Mycobacterium tuberculosis* is highly dependent on the antigen dose. *PLoS One* 4, e5930 (2009)